Quantum chemistry simulations in an undergraduate project

Walker, Bethany; Finlayson, Chris E.

Published in:
European Journal of Physics

DOI:
10.1088/1361-6404/acb9c7

Publication date:
2023

Citation for published version (APA):
Walker, B., & Finlayson, C. E. (2023). Quantum chemistry simulations in an undergraduate project: Tellurophenes as narrow bandgap semiconductor materials. *European Journal of Physics*, *44*(2), [025401]. https://doi.org/10.1088/1361-6404/acb9c7

European Journal of Physics

Quantum chemistry simulations in an undergraduate project: tellurophenes as narrow bandgap semiconductor materials

To cite this article: Bethany Walker and Chris E Finlayson 2023 *Eur. J. Phys.* **44** 025401

OPEN ACCESS
IOP Publishing
European Journal of Physics
Eur. J. Phys. **44** (2023) 025401 (13pp)
https://doi.org/10.1088/1361-6404/acb9c7

Quantum chemistry simulations in an undergraduate project: tellurophenes as narrow bandgap semiconductor materials

Bethany Walker and Chris E Finlayson

Department of Physics, Prifysgol Aberystwyth University, Aberystwyth, Wales SY23 3BZ, United Kingdom

E-mail: cef2@aber.ac.uk

Received 1 September 2022, revised 19 January 2023
Accepted for publication 7 February 2023
Published 2 March 2023

Abstract

The convenient graphical user-interfaces now available with advanced simulation software offer a powerful didactic tool for research-led teaching of methods in quantum chemistry and wider applications of quantum mechanics. In the student project work reported here, a homologous series of semiconducting chalcogenophenes (encompassing poly-thiophenes, poly-selenophenes and poly-tellurophenes) with varying polymer chain lengths were simulated in detail using density functional theory (DFT). Following geometry optimization, energy calculations reveal that increasing the length of the polymer chain (N) from a monomer to a hexamer leads to a narrowing and large-N convergence of the bandgap. It is found that hexa-tellurophene has significantly favourable electronic properties as compared to the other analogues, with a greatly enhanced electron affinity (−2.74 eV), and a corresponding bandgap energy of 2.18 eV, giving a superior matching to the solar spectrum.

Keywords: simulation, graphical user-interface, quantum chemistry, semiconductors, chalcogenophenes, undergraduate projects

(Some figures may appear in colour only in the online journal)

1. Introduction

This paper reports and reflects upon the use of advanced simulation software in the planning and delivery of research-led undergraduate (UG) physics student projects.

0143-0807/23/025401+13$33.00 Printed in the UK

Final year student projects or dissertations are a key element of most UG science degree courses [1], offering the opportunity for students to expand their acquired knowledge and skills towards real-world research areas, under the guidance of academic supervision [2] and also within a peer-team network [3, 4]. In the Department of Physics at Aberystwyth University, students undertake major research-based projects, working in groups of one or two, on elective topics [5]. These projects count for 40 credits at Year 3 level or 60 credits at Year 4 level (representing one-third and one-half of the overall final-year assessment respectively). Reflecting the so-called '3 pillars' of scientific research [6], projects fall into the categories of experiment, theory and simulation, although much overlap between the pillars and some sub-categorisation (e.g. 'instrumentation') may be in evidence. Simulation-based projects offer a particular value, in terms of the efficiency of supervisory time input, and also in developing more open-ended approaches, without the constraints of limited experimental resources and laboratory training requirements.

Electronic structure calculations are an area of biology, chemistry and physics that has seen significant developments in recent decades. The development of computing technology and commercially available simulation software, such as Gaussian [7], has allowed these methods to be increasingly utilised in the research environment. In 1997, only 37 time-dependent density functional theory (TD-DFT) calculations were published, but by 2011 this number had risen to more than 1000 [8].

The widespread current availability and use of commercial/proprietary simulation software within existing university research infrastructures, often involving relatively modest cost investment in comparison to experimental facilities, provides a facile gateway into the educational environment. Additionally, the convenient graphical user-interfaces (GUIs) now available with advanced simulation software offer a powerful didactic tool [9–11] suitable for research-led student projects. This is especially pertinent when familiarising students with the underlying physics and simulation methodologies, whilst not requiring training in higher-level coding and interfacing. Here, we focus on the application of methods in quantum chemistry, allied to the ubiquitous quantum mechanics content, which features so prominently across UG physics curricula [12–14]. Indeed, the topic area is widely viewed as encapsulating many key threshold concepts [15, 16] in the appreciation and understanding of modern physics. As we demonstrate here, the GUI may be used in all relevant aspects of DFT simulation output, including visualisation, energy calculations, and the derived optical spectra.

Semiconducting polymers, or π-conjugated polymers, are an archetypal class of organic materials for the development and improvement of electronic and optoelectronic devices [17, 18]. Since it was discovered in 1977 that iodide-doped polyacetylene [19] was capable of electrical conductivities comparable to those of metals, a discovery that would win the 2000 Nobel Prize in Chemistry, there has been significant research into this class of materials. Uses have spanned organic electronics such as organic light-emitting diodes (OLEDs) [20], organic photovoltaic cells (OPVs) [21], organic field-effect transistors (OFETs) [22] and memory devices [23]. The primary benefits of these π-conjugated semiconducting organic polymers are their easy and cheap synthesis, high electron and hole mobilities, and the ability to tune their band gap by altering the structure and composition of the polymer [24].

The properties of a molecular semiconductor are determined primarily by the energies of the HOMO (highest occupied molecular orbital) and LUMO (lowest unoccupied molecular orbital), and the difference between these two, known as the 'bandgap' (BG). A schematic of the energetics of molecular orbitals in this context is given in figure 1. In any solar cell or OPV, a narrow bandgap and broad light absorption spectrum, with high oscillator strength (or extinction coefficient) [25], is conducive to effective absorption of the available incident light

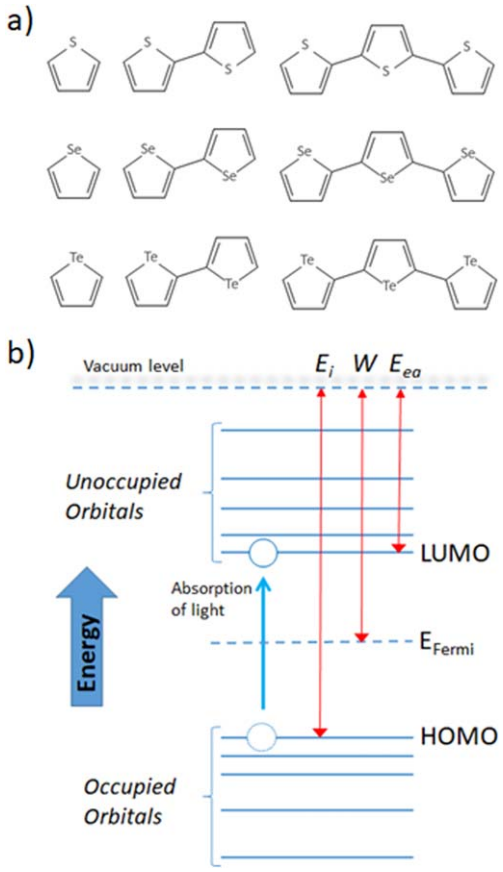

Figure 1. (a) The monomers, dimers, and trimers (L–R) of polythiophene, polyselenophene, and polytellurophene (T–B). (b) Schematic energy level diagram for a molecular semiconductor, illustrating the concepts of HOMO (highest occupied molecular orbital), LUMO (lowest unoccupied molecular orbital), Fermi energy, ionisation energy (E_i), workfunction (W), electron affinity (E_{ea}). The bandgap energy is defined as the difference between the HOMO and LUMO levels.

[26]. For example, if a semiconducting polymer has a bandgap of 3 eV, it will not be able to absorb photons of energies less than 3 eV. Since the bulk of the power density of visible light is within the range of 2.00–2.75 eV [27], a semiconductor of this bandgap would not be suitable for use in a polymer solar cell. Additionally, dependent on the donor or acceptor roles played by materials within a multi-component ('heterojunction') device [28, 29], it may be desirable to have a low-lying LUMO giving higher electron affinity, or a high-lying HOMO giving lower ionisation energy, for example.

An important aspect of this study is to highlight how the achievements and inputs of the UG student (as primary author) connect the pedagogical and scientific elements of the project. Within the stated spirit of research-led projects, the student independently chose and devised this project from the original remit of 'Computational Simulations of Organic Semiconductors', following on from an assignment literature review. The student created all the input files and structures, performed all the simulations, and carried out the majority of the results and analyses reported in the following sections.

This report is concerned with three particular materials belonging to the homologous series of π-conjugated polymers known as poly-chalcogenophenes [30–33]. It can be seen from figure 1(a) that there are contiguous atoms in the polymer backbone, with alkyl-connected heterocyclic units, leading to π-conjugation. The electrons within this system are known as 'π electrons' to distinguish them from electrons forming single bonds. These so-called π electrons become delocalised across all of the overlapping atomic p-orbitals leading to the conducting (or semiconducting) property of the molecules. Polythiophene, polyselenophene, and polytellurophene are polymers containing sulphur, selenium, and tellurium respectively. These three elements are all within group VI of the periodic table, with S, Se, and Te being in periods III, IV, and V respectively. The trend in the electronegativities of these three elements going down group VI (2.58, 2.55, and 2.10 respectively [32]) would suggest a narrowing bandgap from polythiophene to polyselenophene to polytellurophene [31].

In this report, the aforementioned different poly- and oligo-chalcogenophenes are compared and contrasted, increasing the chain length (N) from single monomer units up to $N = 6$ hexamers. The effects of substituent variation, as well as polymer chain length, on the predicted properties of the semiconducting polymers are determined. To facilitate this investigation, the proprietary software Gaussian 09 is utilised [34]. This software allows for DFT (density functional theory) calculations to be made of the energetically optimised geometry of the molecules, and subsequently calculations of the electronic orbitals, HOMO and LUMO energies, and bandgaps energies. Additionally, other electronic characteristics of the polymers can then be determined, such as the optical absorption spectra and oscillator strength, and visualisation of the orbital wavefunctions. Geometry optimization and energy calculations reveal that increasing N from 1 to 6 (monomer to hexamer) leads to a narrowing and large-N convergence of the bandgap. It is found that hexa-tellurophene has significantly favourable electronic properties as compared to the other analogues, with a greatly enhanced electron affinity (-2.74 eV), and a corresponding bandgap energy of 2.18 eV, giving a superior matching to the solar spectrum.

2. Methods

In this investigation, a Linux-based version of the Gaussian 09 software [34], as accessed by the Gaussview GUI [35], is used to simulate the optimised geometries, bandgap, excitation energy, HOMO, LUMO, oscillator strength, and absorption spectrum for each molecule under study.

2.1. Geometry optimisation

The first step of the simulation is the geometry optimisation calculation, which employs an example of a so-called variational approach [36], whereby the eigen-energy associated with a quantum mechanical system is iteratively minimized with respect to one or more variables.

Here, the calculation attempts to predict the positioning of all the atoms and bonds within the molecule at a minimum energy. The geometry of the molecule at a minimum energy is typically how the geometry of the molecule would be found in its ground state, except in cases where entropic constraints contribute substantially to the overall free energy. This is achieved by finding the place at which the energy with respect to the positioning of the nuclei differentiates to zero, so the net force acting on the nuclei within the molecule is zero. The geometry of the molecule is changed until a saddle point on the potential energy surface (the energy of the system expressed in terms of the positioning of the atoms) is determined. This

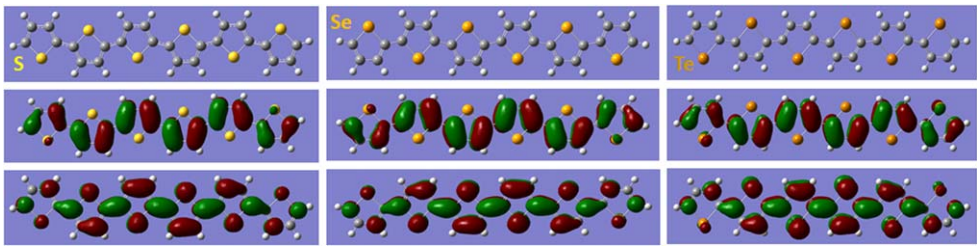

Figure 2. Optimized geometries of hexamers of thiophene, selenophene, and tellurophene are shown top (L–R, as indicated). The atoms are coloured as S—yellow, Se—orange, Te—brown, C—grey, H—white. (T–B) Corresponding simulated HOMO and LUMO spatial orbitals are shown, with electron density (surface isovalue probability of 0.0004 e $Å^{-3}$) illustrated by the green and red lobes of alternate wavefunction phase.

then becomes optimised geometry of the molecule and is used as the structure on which to perform the subsequent energy calculations.

For the geometry optimisation and subsequent simulations, DFT (density functional theory) is used; examples of such optimised geometries are shown in figure 2 for thiophene, selenophene and tellurophene hexamers. Of note is the conformal planarity of all these structures, with the entirety of the conjoined aromatic rings being coplanar within the 2D plane of view.

2.1.1. Density functional theory; functionals and basis sets. There are several methods of quantum calculation starting from the molecular Hamiltonian, all of which have their drawbacks. Hartree–Fock (HF), Møller-Plesset perturbation theory (MP), configuration interaction (CI), and density functional theory (DFT) all build upon one another to improve the accuracy of the calculations. HF is the least accurate of these methods since the interactions between the electrons in the system are treated approximately. HF is therefore often sufficient for a single electron system, but becomes problematic and is not accurate enough when applied to larger systems, and other methods are preferred. The perturbative corrections of MP and CI develop on HF by providing more accurate electronic energies, but again only for smaller systems. HF, MP and CI all rely on the direct computation of the wavefunction of the atom or molecule, and they generally lose efficacy and accuracy for larger systems.

DFT is the preferred method for systems containing many electrons. It does not rely on the computation of the wavefunction of the molecule, but instead it uses the total electron density of the molecule. DFT can therefore provide a significantly improved accuracy and generally lower computation costs than the previous methods [37].

In DFT, the total energy of the system is thought of as a function of the electron density of the system, which speeds up the calculation rather than using the wavefunction directly. The increase in popularity of DFT has led to a constantly improving selection of functionals available for approximating the electron density. Modern DFT functionals are computationally faster and require less disc space [38]. One of the most popular functionals if the B3LYP (Becke, 3-parameter, Lee–Yang–Parr) exchange-correlation hybrid functional:

$$E_{xc}^{\mathrm{B3LYP}} = (1 - a)E_x^{\mathrm{LSDA}} + aE_x^{\mathrm{HF}} + b\Delta E_x^b + (1 - c)E_c^{\mathrm{LSDA}} + cE_c^{\mathrm{LYP}}, \quad (1)$$

where $a = 0.20$, $b = 0.72$, $c = 0.81$. These three parameters are used to combine the Hartree–Fock exchange-correlation function, an exact calculation, (E_x^{HF}), the LYP correlation functional (E_c^{LYP}), a gradient approximation (E_x^b), and the local spin density approximation (E_c^{LSDA}) with different weightings. It offers a good trade-off between computational cost and accuracy. This robustness and simplicity of this function having relatively few parameters compared to as many as 26 in other functionals [39], making it the most popular functional in DFT calculations [40].

Another important component of DFT is the basis set used. The basis set is a set of functions representing the electronic wavefunction within an appropriate spatial coordinate system. The choice of basis set will determine the accuracy of the results, since basis functions are specialised for certain systems, often accounting for any characteristic symmetries. The choice will also affect the computational time cost of the calculations, since some basis sets are larger and more complex than others. For molecular systems such as those involving large polymers or macromolecules, basis sets composed of Gaussian-type functions are often utilised, with the functions taking the form [41]:

$$\chi(\zeta, n, m, l: r, \theta, \phi) = NY_{l,m}(\theta, \phi)r^{2n-2-l}\mathrm{e}^{-\zeta r^2}, \quad (2)$$

where N is the normalisation constant, ζ is the exponent, $Y_{l,m}$ are spherical harmonic functions, and n, m, and l correspond to the type of orbital (s, p, or d, for example). A linear combination of these functions are taken to form the basis set, of the form [41]:

$$\varphi = \sum_i n_i \chi_i, \quad (3)$$

where n_i is the contraction coefficient. It is again often necessary to compromise with basis sets, as with functionals. Larger basis sets will provide a greater degree of accuracy, but at a greater computational cost and time. Usually smaller basis sets, such as the commonly used 6–31G basis set, which provides reliable results for large carbon structures [42], are sufficient, and the use of a larger basis set will not improve the accuracy sufficiently to justify the additional computation cost and time.

For the polythiophenes and polyselenophenes in this study, the B3LYP functional and the 6–31G basis set are used unless otherwise stated. The geometry of the polytellurophenes is also optimised using the B3LYP functional, but the larger Def2-SVP basis set is employed since it is more suitable for heavier elements [43].

2.2. Energetics calculations

The second and final step of the simulation is the energy calculation, leading to the orbital energies and optical transition characteristics for each polymer. For the simulations, it is necessary to specify a level of theory, a function, and a basis set.

Following geometry optimisation, TD-SCF (time-dependent, self-consistent field) is the DFT method used to perform the energy calculation, but the density functionals and basis sets specified above for each class of polymer homologue remain the same. Since polythiophene contains the lightest element of the three classes of polymer under investigation (sulphur, compared to selenium and tellurium), the first molecules simulated are polythiophenes, beginning with the simplest (monomer) structure. This is then extended to the dimer, trimer and so on of all three homologues, until the band gap of the polymer chain begins to converge, therefore providing an accurate enough estimation of the electronic properties. The

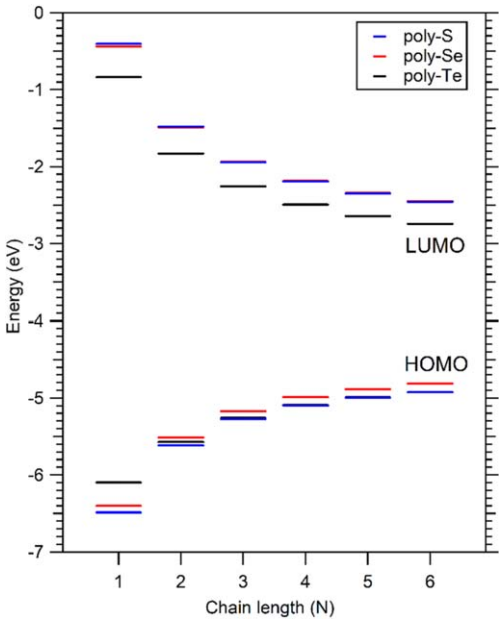

Figure 3. The HOMO (highest occupied molecular orbital) and LUMO (lowest unoccupied molecular orbital) of polythiophene (poly-S), polyselenophene (poly-Se), and polytellurophene (poly-Te), plotted against the length of the polymer chain (degree of polymerisation, *N*).

excitation energy of the lowest excited state $E(N)$ can be approximately expressed in terms of the N degree of polymerisation by the following equation [44]:

$$E(N) = E_{\infty} + (E_1 - E_{\infty})\mathrm{e}^{-a(N-1)}, \tag{4}$$

where N is the degree of polymerisation (polymer chain length), E_1 and E_{∞} are the measured excitation energies for the polymer and monomer respectively, and a is a parameter which describes the speed at which $E(N)$ will converge towards E_{∞}. This equation demonstrates how the excitation energy, an important characteristic in determining the performance and suitability of a semiconducting polymer for a given application, may be engineered by changing the length of the polymer chain.

A pragmatic trade-off is required to ensure the computational time and storage space used up by the simulations are not too large, and that the work planned for the project can be completed within a realistic time. Ideally, the length of the polymer chain would very large, to ensure the band gap converges as closely as possible on the true value of the band gap at the large-N limit. However, it is expected that the length of time of the simulations will increase as a strong (approximately exponential) function of increasing chain length [45, 46]. On a similar note, the sidechains and moiety structures associated with organic molecules and polymers may add a significant computational cost, whilst not contributing directly to the π-orbital structure. Simplification of structures, including the shortening of alkyl sidechains to simple H-termination is therefore employed by convention [47, 48].

Once the length of the polymer chain providing a sufficiently accurate value of the band gap has been determined for thiophenes, these simulation strategies are repeated for selenophenes, and tellurophenes; thus, giving a complete picture of the homologous series and chain length variations associated with the poly-chalcogenophenes under study.

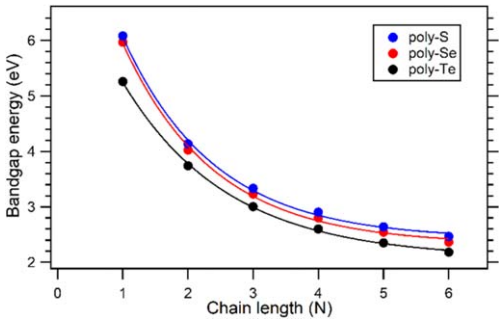

Figure 4. The simulated bandgap of polythiophene (poly-S), polyselenophene (poly-Se), and polytellurophene (poly-Te), potted against the length of the polymer chain (degree of polymerisation).

2.3. Orbital visualisation

As illustrated in figure 2, the GUI enables direct spatial visualisation of the simulated HOMO and LUMO orbital levels of molecules (and indeed other calculated states). These rendered images of the 3D electronic density distributions allow the symmetries and shapes of molecular orbitals to be qualitatively ascertained. 'Surfaces' are generated corresponding to iso-values of electron probability ($|\psi^2|$) density, with alternate wavefunction phases denoted by the green and red lobes; these colours do not, therefore, correspond to alternate charges or polarities, as is sometimes misrepresented.

We can see from figure 2 that both LUMO and HOMO levels are π-orbitals extended symmetrically across the conjugated backbone of the molecule, whilst having very different characteristic shape geometries.

3. Results

As an integral part of assessment, the UG student completed a formal report/dissertation and also a short peer-group presentation. This section uses these student outputs as the template in presenting the main project results.

Figure 3 shows the key outputs of HOMO and LUMO energies, plotted again the length of the polymer chain (N) starting at the monomer for polythiophene (poly-S), polyselenophene (poly-Se), and polytellurophene (poly-Te). We estimate the global uncertainty for the HOMO, LUMO values from the simulations as ± 0.1 eV [49], given the functional and basis set used here within DFT to approximate the electron density and the electronic wavefunction respectively.

All three monomers display a lower-lying HOMO, as compared to the dimers and the trimers, with the HOMO increasing and converging with increasing polymer chain length. It can be seen that there is little variation in terms of HOMO position over the chain lengths up to $N = 6$. The poly-S monomer starts with the lowest-lying HOMO, and poly-Te with the highest, but with increasing chain length poly-S and poly-Te converge towards parity, with poly-Se having a marginally more high-lying HOMO for chains of length $N = 2$ or greater.

Figure 3 also shows the trend of LUMO values against the length of the polymer chain. There are much greater differences between the three homologues than for the HOMO levels. For chains of all lengths, poly-Te shows a low-lying LUMO which is some 0.3–0.5 eV lower than for poly-S and poly-Se, which have almost identical values up to $N = 6$. This is of

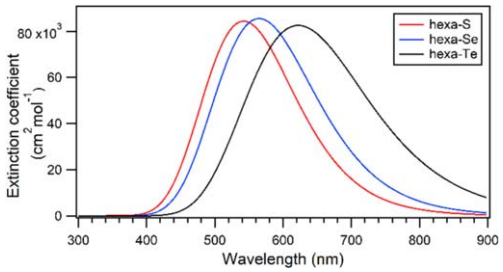

Figure 5. The absorption spectra of the hexamers of polythiophene, polyselenophene, and polytellurophene.

Table 1. Extrapolated LUMO, HOMO and bandgap energies as calculated for the polychalcogenophenes as indicated. Also shown are the excitation wavelength, spectral range (as defined) and absorption oscillator strength, as inferred from the hexamer simulations.

	Poly-S	Poly-Se	Poly-Te
LUMO (eV)	−2.44	−2.45	−2.74
HOMO (eV)	−4.92	−4.81	−4.92
Bandgap (eV)	2.421	2.322	2.073
Excitation λ (nm)	542.2	564.8	622.2
Spectral range (nm)	95.6	103.6	128.7
Oscillator strength	2.083	2.110	2.037

particular significance in reference to the energetics of many common electroactive materials used in heterojunction devices such as PCBM (Phenyl-C61-butyric acid methyl ester) [50].

The bandgap, which is calculated as the difference between the HOMO and LUMO energy values plotted in figure 3, is displayed in figure 4 for all analogues going up to $N = 6$. These data show a clear trend at all N going from poly-S to poly-Se to poly-Te of a decreasing bandgap magnitude; this narrowing of the gap is also more marked between poly-Se and poly-Te compared to that between poly-S and poly-Se. The total variance in the bandgap is greatest for smaller chain lengths (of order 1 eV), with the difference in the band gap decreasing with increasing chain length (of order 0.5 eV at $N = 6$).

The transition oscillator strengths, as ascertained from the calculated HOMO and LUMO wavefunctions of the hexamers are given in table 1. Poly-S and poly-Se show almost identical values, with the oscillator strength increasing linearly with increasing chain length. Poly-Te displays the same trend but has a value that is a few % smaller at each N.

By taking into account both the predicted optical transitions between HOMO-LUMO levels and their associated oscillator strengths, the absorption spectra of the three homologues are modelled in figure 5 (chain lengths of $N = 6$). Each of these hexamers show peak absorption in the visible region of the spectrum. Commensurately, excitation energies corresponding to the peak of the absorption spectra may be extracted (table 1). As is consistent with the calculated electronic bandgap, poly-Te shows a considerable red-shifting compared to poly-Se and poly-S; spectral shifts of 58 and 80 nm respectively. A measure of the spectral range may also be determined from the full-width-half-maximum (FWHM). The spectrum of poly-Te is significantly broader and encompasses a greater range than poly-S and poly-Se (table 1), as is readily verified qualitatively from figure 5.

Finally, extrapolation of the data points in figure 4, using the mathematical formulism of equation (4), enables us to ascertain the polymer chain (large-N) values of the semiconductor bandgap for poly-S, poly-Se and poly-Te, results which are given in table 1 as 2.421, 2.322, and 2.073 eV respectively. At the level of qualitative trends, these may be compared with literature values in experimental determinations [31, 51, 52]. Likewise, an exponential extrapolation of the HOMO and LUMO values in figure 3 gives a notional large-*N* value, as displayed in table 1. The much-increased electron affinity (LUMO) of poly-Te is again highlighted, being some 0.3 eV lower than the other two homologues.

4. Discussion and conclusions

The purpose of this student major project 'Computational Simulations of Organic Semiconductors' was to simulate polythiophenes, polyselenophenes, and polytellurophenes to determine which of these polymers has the most favourable electronic, optical and optoelectronic properties, as well as determining the effect of the degree of polymerisation (N), ranging from the monomers to oligomers and to polymers in the large-*N* limit.

These aims were accomplished by using Gaussian 09 software to carry out geometry optimisation simulations on the polymers. These simulations determined the geometry of the polymer at a minimum energy, which would correspond to how the polymer would naturally occur in a free-space environment. Once the optimised geometry had been determined, an energy calculation was carried out using density functional theory on the optimised geometry. This calculation provided the HOMO (highest occupied molecular orbital), LUMO (lowest unoccupied molecular orbital), oscillator strength, excitation energy, band gap, and absorption spectrum of the molecule.

Polymers were simulated of poly-S, poly-Se, and poly-Te of increasing degrees of polymerisation. Starting with the monomer, and eventually building up to a polymer of length six (hexamer). From the data gathered from these simulations, the monomers had the largest band gap, but the values decreased and converged with increasing polymer chain length.

It is evident across this study that, of the three poly-chalcogenophenes homologues, polytellurophene shows the most favourable electronic properties, having the lowest-lying LUMO (largest electron affinity). Poly-Te also has the smallest magnitude bandgap and the broadest absorption spectrum, giving an enhanced matching with the solar spectrum. These properties are useful in various optoelectronics applications, particularly in solar cells and photovoltaics, where a narrow band gap and a broad absorption spectrum allows for as much light absorption as possible [53–55]. These more favourable properties may be attributed to numerous factors related to the electronic structure, the decreased electronegativity, and bonding polarisation behaviour of tellurium in such conjugated organic molecules [32]. As a caveat of note, the intermolecular interactions between Te atoms, which are notionally stronger than those between Se and S atoms, may further influence variations in properties beyond the intramolecular scope of the study here [33, 56].

These results support and augment the reports in the literature surrounding this topic, both in theory and experiment, suggesting that the relatively under-explored polytellurophenes may be an advantageous substitute to polythiophenes and polyselenophenes, owing to these superior electronic and optoelectronic properties. In particular, we hope for renewed and accelerated efforts to facilitate synthesis of the kinds of organo-tellurium compounds [51, 52, 57, 58] to enable further characterisation in real-world applications.

This paper illustrates the adaptation of commercially available simulation software for use in an undergraduate final-year project on quantum chemistry. The report demonstrates the

possibilities of substantive research outputs from such open-ended projects, notwithstanding the clear educational and pedagogical goals and benefits. GaussView offers an exemplary accessible graphical user-interface for research-led student projects, encapsulating many important curriculum areas and threshold concepts. The pedagogical and scientific elements of the project are interconnected with the achievements and inputs of the UG student; work for which a departmental prize was awarded.

We give a final mention to the ongoing software development in this area, commensurate with the rapid growth in computing technology, power and networking within university research infrastructures. Since the project was completed in May 2022 and partly based on the success of this and other research projects, the University has invested in the Gaussian 16 version upgrade [59]. Continuing in the 40-odd year progression of the *Gaussian* series of electronic structure programs, this offers capabilities to study even larger molecular systems beyond the oligomers featured in this paper. The latest GUI, GaussView 6, also offers an enriched set of building and visualization capabilities. We thus anticipate offering many more such opportunities for UG simulation projects aligned with active and prescient research programmes.

Acknowledgments

The authors thank Dr Alun Jones and Dr Edwin Flikkema of Aberystwyth University for technical advice.

Data availability statement

The data that support the findings of this study are available upon reasonable request from the authors.

ORCID iDs

Chris E Finlayson https://orcid.org/0000-0002-9068-7584

References

[1] Exley K 1999 Key Aspects of Teaching and Learning in Science and Engineering *Handbook for Teaching and Learning in Higher Education.* (London: Kogan Page) Chap. 20
[2] Finlayson C E 2014 *Postgraduate Certificate for Teaching in Higher Education (PGCTHE)* (UK: Aberystwyth University) (http://hdl.handle.net/2160/e2e6fb7d-72cf-49be-a82e-e97ddfb34627)
[3] Collier K G 1980 Peer-group learning in higher-education—the development of higher-order skills *Studies Higher Educ.* **5** 55–62
[4] Boud D, Cohen R and Sampson J 1999 Peer learning and assessment *Assessment Evaluation Higher Educ.* **24** 413–26
[5] http://aber.ac.uk/en/phys/prospective/, https://aber.ac.uk/en/phys/study-with-us/undergrad/ 16th Feb 2023
[6] Skuse B 2019 The third pillar *Phys. World* **32** 40–3
[7] https://gaussian.com/
[8] Adamo C and Jacquemin D 2013 The calculations of excited-state properties with time-dependent density functional theory *Chem. Soc. Rev.* **42** 845–56
[9] Hattie J 2012 *Visible Learning for Teachers* (Abingdon, UK: Routledge)
[10] Teixeira E S, Maria Greca I and Freire O Jr 2012 The history and philosophy of science in physics teaching: a research synthesis of didactic interventions *Sci. Educ.* **21** 771–96

[11] Berglund A and Lister R 2010 Introductory Programming and the Didactic riangle *Proc. 12th Australasian Computing Education Conf. (ACE 2010)* Vol. 103 (Brisbane, Australia: Australian Computer Society, Inc.) pp 35–44
[12] Krijtenburg-Lewerissa K, Pol H J, Brinkman A and van Joolingen W R 2017 Insights into teaching quantum mechanics in secondary and lower undergraduate education *Phys. Rev. Phys. Educ. Res.* **13** 21
[13] Greca I M and Freire O 2014 Teaching introductory quantum physics and chemistry: caveats from the history of science and science teaching to the training of modern chemists *Chem. Educ. Res. Pract.* **15** 286–96
[14] Cataloglu E and Robinett R W 2002 Testing the development of student conceptual and visualization understanding in quantum mechanics through the undergraduate career *Am. J. Phys.* **70** 238–51
[15] Meyer J H F and Land R 2005 Threshold concepts and troublesome knowledge (2): Epistemological considerations and a conceptual framework for teaching and learning *Higher Educ.* **49** 373–88
[16] Milner-Bolotin M, Antimirova T, Noack A and Petrov A 2011 Attitudes about science and conceptual physics learning in university introductory physics courses *Phys. Rev. ST Phys. Educ. Res.* **7** 020107
[17] Luscombe C K, Maitra U, Walter M and Wiedmer S K 2021 Theoretical background on semiconducting polymers and their applications to OSCs and OLEDs *Chem. Teacher Int.* **3** 169–83
[18] Osaka I 2015 Semiconducting polymers based on electron-deficient pi-building units *Polym. J.* **47** 18–25
[19] Chiang C K, Fincher C R, Park Y W, Heeger A J, Shirakawa H, Louis E J, Gau S C and Macdiarmid A G 1977 Electrical-conductivity in doped polyacetylene *Phys. Rev. Lett.* **39** 1098–101
[20] Kamtekar K T, Monkman A P and Bryce M R 2010 Recent advances in white organic light-emitting materials and devices (WOLEDs) *Adv. Mater.* **22** 572–82
[21] Nguyen T L *et al* 2014 Semi-crystalline photovoltaic polymers with efficiency exceeding 9% in a similar to 300 nm thick conventional single-cell device *Energy Environ. Sci.* **7** 3040–51
[22] Sirringhaus H 2005 Device physics of solution-processed organic field-effect transistors *Adv. Mater.* **17** 2411–25
[23] Lin H W, Lee W Y and Chen W C 2012 Selenophene-DPP donor-acceptor conjugated polymer for high performance ambipolar field effect transistor and nonvolatile memory applications *J. Mater. Chem.* **22** 2120–8
[24] Li M M, Leenaers P J, Wienk M M and Janssen R A J 2020 The effect of alkyl side chain length on the formation of two semi-crystalline phases in low band gap conjugated polymers *J. Mater. Chem. C* **8** 5856–67
[25] Hecht E 2002 *Optics* 4th edn (San Francisco, CA: Pearson Education)
[26] Gao F, Wang Y, Shi D, Zhang J, Wang M K, Jing X Y, Humphry-Baker R, Wang P, Zakeeruddin S M and Gratzel M 2008 Enhance the optical absorptivity of nanocrystalline TiO (2) film with high molar extinction coefficient ruthenium sensitizers for high performance dye-sensitized solar cells *JACS* **130** 10720–8
[27] Lee T D and Ebong A U 2017 A review of thin film solar cell technologies and challenges *Renew. Sustain. Energy Rev.* **70** 1286–97
[28] McNeill C and Greenham N 2009 Conjugated-polymer blends for optoelectronics *Adv. Mater.* **21** 3840–50
[29] McNeill C, Abrusci A, Zaumseil J, Wilson R, McKiernan M, Burroughes J, Halls J, Greenham N and Friend R 2007 Dual electron donor/electron acceptor character of a conjugated polymer in efficient photovoltaic diodes *Appl. Phys. Lett.* **90** 193506
[30] Lin H W, Lee W Y, Lu C, Lin C J, Wu H C, Lin Y W, Ahn B, Rho Y, Ree M and Chen W C 2012 Biaxially extended quaterthiophene-thiophene and selenophene conjugated polymers for optoelectronic device applications *Polym. Chem.* **3** 767–77
[31] Topolskaia V, Pollit A A, Cheng S and Seferos D S 2021 Trends in conjugated chalcogenophenes: a theoretical study *Chem. Eur. J.* **27** 9038–43
[32] Patra A and Bendikov M 2010 Polyselenophenes *J. Mater. Chem.* **20** 422–33

[33] Manion J G, Ye S Y, Proppe A H, Laramee A W, McKeown G R, Kynaston E L, Kelley S O, Sargent E H and Seferos D S 2018 Examining structure-property-function relationships in thiophene, selenophene, and tellurophene homopolymers *ACS Appl. Energy Mater.* **1** 5033–42
[34] Frisch M J *et al* (2016) Gaussian 09, Revision E.01.Wallingford CT, USA, Gaussian, Inc.
[35] https://gaussian.com/gaussview6/
[36] Ekeland I 1974 Variational principle *J. Math. Anal. Appl.* **47** 324–53
[37] Baseden K A and Tye J W 2014 Introduction to density functional theory: calculations by hand on the helium atom *J. Chem. Educ.* **91** 2116–23
[38] Kristyan S 1995 Note on the choice of basis-set in density-functional theory calculations for electronic-structures of molecules (test on the atoms from the first 3 rows of the periodic-table (2-less-than-or-equal-to-n-less-than-or-equal-to-Z-less-than-or-equal-to −18), water, ammonia and pyrrole) *Chem. Phys. Lett.* **247** 101–111
[39] Tirado-Rives J and Jorgensen W L 2008 Performance of B3LYP density functional methods for a large set of organic molecules *J. Chem. Theory Comput.* **4** 297–306
[40] Becke A D 1993 Density-functional thermochemistry .3. the role of exact exchange *J. Chem. Phys.* **98** 5648–52
[41] Hill J G 2013 Gaussian basis sets for molecular applications *Int. J. Quantum Chem.* **113** 21–34
[42] Wang H, He Y, Li Y and Su H 2012 Photophysical and electronic properties of five PCBM-like C-60 derivatives: spectral and quantum chemical view *J. Phys. Chem. A* **116** 255–62
[43] Weigend F 2006 Accurate Coulomb-fitting basis sets for H to Rn *Phys. Chem. Chem. Phys.* **8** 1057–65
[44] Rissler J 2004 Effective conjugation length of pi-conjugated systems *Chem. Phys. Lett.* **395** 92–6
[45] Yassar A, Roncali J and Garnier F 1989 Conductivity and conjugation length in poly(3-methylthiophene) thin-films *Macromolecules* **22** 804–9
[46] Jones M A, Vallury H J, Hill C D and Hollenberg L C L 2022 Chemistry beyond the Hartree–Fock energy via quantum computed moments *Sci. Rep.* **12** 9
[47] Lu L, Finlayson C, Kabra D, Albert-Seifried S, Song M, Havenith R, Tu G, Huck W and Friend R 2013 The influence of side-chain position on the optoelectronic properties of a red-emitting conjugated polymer *Macromol. Chem. Phys.* **214** 967–74
[48] Oliveira E F and Lavarda F C 2014 Effect of the length of alkyl side chains in the electronic structure of conjugated polymers *Mater. Res.-Ibero-Am. J. Mater.* **17** 1369–74
[49] Weigend F and Ahlrichs R 2005 Balanced basis sets of split valence, triple zeta valence and quadruple zeta valence quality for H to Rn: Design and assessment of accuracy *Phys. Chem. Chem. Phys.* **7** 3297–305
[50] Oliveira E F and Lavarda F C 2014 Molecular design of new P3HT derivatives: Adjusting electronic energy levels for blends with PCBM *Mater. Chem. Phys.* **148** 923–32
[51] Nishiyama H, Zheng F, Inagi S, Fueno H, Tanaka K and Tomita I 2020 Tellurophene-containing pi-conjugated polymers with unique heteroatom-heteroatom interactions by post-element-transformation of an organotitanium polymer *Polym. Chem.* **11** 4693–8
[52] Wu X X, Lv L, Hu L F, Shi Q Q, Peng A D and Huang H 2019 The synthesis and optoelectronic applications for tellurophene-based small molecules and polymers *Chem. Phys. Chem.* **20** 2600–7
[53] Scharber M C and Sariciftci N S 2021 Low band gap conjugated semiconducting polymers *Adv. Mater. Technol.* **6** 9
[54] Liu X F, Sun Y M, Hsu B B Y, Lorbach A, Qi L, Heeger A J and Bazan G C 2014 Design and properties of intermediate-sized narrow band-gap conjugated molecules relevant to solution-processed organic solar cells *JACS* **136** 5697–708
[55] Chang C C, Chen C P, Chou H H, Liao C Y, Chan S H and Cheng C H 2013 New selenophene-based low-band gap conjugated polymers for organic photovoltaics *J. Polym. Sci.* A **51** 4550–7
[56] Rodewald M, Rautiainen J M, Niksch T, Gorls H, Oilunkaniemi R, Weigand W and Laitinen R S 2020 Chalcogen-bonding interactions in telluroether heterocycles Te(CH2)(m) (n)(n = 1–4; m = 3–7) *Chem. Eur. J.* **26** 13806–18
[57] Rhoden C R B and Zeni G 2011 New development of synthesis and reactivity of seleno- and tellurophenes *Org. Biomol. Chem.* **9** 1301–13
[58] Rivard E 2015 Tellurophenes and their emergence as building blocks for polymeric and light-emitting materials *Chem. Lett.* **44** 730–6
[59] https://gaussian.com/gaussian16/